

# Syno: Structured Synthesis for Neural Operators

Yongqi Zhuo\*  
 Tsinghua University  
 Beijing, China  
 zhuoyq21@mails.tsinghua.edu.cn

Chenggang Zhao  
 Tsinghua University  
 Beijing, China  
 zhaocg21@mails.tsinghua.edu.cn

Zhengyuan Su\*  
 Tsinghua University  
 Beijing, China  
 su-zy21@mails.tsinghua.edu.cn

Mingyu Gao  
 Tsinghua University  
 Beijing, China  
 gaomy@tsinghua.edu.cn

## Abstract

The desires for better prediction accuracy and higher execution performance in neural networks never end. Neural architecture search (NAS) and tensor compilers are two popular techniques to optimize these two goals, but they are both limited to composing or optimizing existing manually designed operators rather than coming up with completely new designs. In this work, we explore the less studied direction of neural operator synthesis, which aims to automatically and efficiently discover novel neural operators with better accuracy and/or speed. We develop an end-to-end framework Syno, to realize practical neural operator synthesis. Syno makes use of a novel set of fine-grained primitives defined on tensor dimensions, which ensure various desired properties to ease model training, and also enable expression canonicalization techniques to avoid redundant candidates during search. Syno further adopts a novel guided synthesis flow to obtain valid operators matched with the specified input/output dimension sizes, and leverages efficient stochastic tree search algorithms to quickly explore the design space. We demonstrate that Syno discovers better operators with an average of  $2.06\times$  speedup and less than 1% accuracy loss, even on NAS-optimized models.

**Keywords:** Machine Learning, Program Synthesis, Neural Architecture Search

## 1 Introduction

Deep learning with neural networks (NNs) has been a surprisingly effective algorithm breakthrough to handle many challenging tasks in various domains. Since its emergence in the last decade, people have been continuously seeking to improve both the quality (in terms of, e.g., prediction accuracy) and the performance (in terms of training and inference time) of NN models, in order to adapt them to more complicated real-world scenarios with lower computational cost.

Two complementary research paradigms have been developed. To systematically design new NN models with better accuracy quality, neural architecture search (NAS) [8, 20,

42, 43] uses deep learning algorithms themselves to automatically discover promising model structures [28–30, 37]. Given a backbone network topology, NAS explores how to construct the basic cells in the model using combinations of basic operators like convolutions and pooling. The optimization goal is either pure accuracy, or a balance between accuracy and speed [2, 3, 29, 37]. In contrast, to improve training and inference speeds, tensor compilers [5, 24, 36, 39, 40] aim to optimize the implementation of low-level loop nests of each operator in an NN model. Various general and specialized compile-time optimizations are applied to the operator, without altering its functional semantics.

We notice that a new direction orthogonal to the above two has not been fully explored, namely to *synthesize novel neural operators at a fine granularity*, with the goal to automatically and efficiently discover new operators beyond existing standard types (e.g., convolutions), to improve accuracy quality and/or execution performance. NAS only composes its cell structures using *existing* operators, and tensor compilers only explore *semantically equivalent* variants of the original operators. We envision that these three complementary approaches could be used together. For example, starting from a NAS-discovered network topology, we synthesize novel operators to replace the original ones in the model, and finally leverage tensor compilers to optimize their execution speeds on specific hardware backends.

Neural operator synthesis can be viewed as a domain-specific form of program synthesis [11], a classic topic in computer science. Generic program synthesis approaches face the issues of scalability and misaligned correctness targets. Early attempts of program synthesis for NNs [17, 21] are still limited to composing with coarse-grained basic operators and leave large potential gains unexploited. More specifically, to explore a sufficiently large design space, *fine-grained synthesis* that composes directly from the very basic programming language atoms is ideally desired. This is a highly challenging task. First, the arbitrarily composed candidates would be very unlikely to satisfy the common properties of neural operators, such as differentiability, no replication or discard of tensor elements, etc. Second, there will be enormous redundancy in the synthesized operator

\*Both authors contributed equally to the paper

candidates with the same and similar semantics. Such equivalent semantics are already efficiently explored by tensor compilers, so we want to prune them out and focus on discovering new operators. Finally, program synthesis has complicated search spaces, and neural operators have the unique search goal of accuracy, different from the strict and clear correctness requirement in traditional synthesis. A new search method is thus needed.

We develop *an end-to-end, automatic, and efficient neural operator synthesis framework*, Syno. It takes a given backbone NN topology, and searches for novel linear operators to replace the original ones in the model, in order to improve prediction accuracy and/or execution performance. Syno addresses the aforementioned challenges with several key techniques. First, it makes use of a novel set of *fine-grained primitives* to synthesize new operators. The primitive semantics are defined on tensor coordinates (i.e., dimensions). They maintain tensor semantics and exhibit high-quality properties for neural operators, while not sacrificing expressiveness. Second, Syno leverages *expression simplification and canonicalization* techniques to analyze and eliminate most of the redundancies when synthesizing operators, especially to avoid redoing tensor compiler optimizations. Finally, the design space search process is made more structured, which iteratively samples and adds new primitives to compose operator candidates. We formulate it as a Markov decision process and leverage the efficient *Monte Carlo Tree Search* algorithm [6, 9, 13]. We further propose a novel metric of *shape distance* to guide the synthesis towards matching with the required input/output tensor shapes, so that the operator candidate is valid to be used in the backbone model. The discovered operators use two dedicated code generators to evaluate their accuracy and speed, respectively.

Evaluated on five vision models and GPT-2, Syno discovers faster operators than standard convolution and matrix multiplication, even on NAS-optimized backbone models. Within 1% accuracy loss on CIFAR-100, using Syno-optimized operators exhibits up to  $3.41 \times$  ( $2.66 \times$ ) speedups and  $2.06 \times$  ( $1.72 \times$ ) on average compared to the original models, targeting mobile CPUs (GPUs). On ImageNet, they achieve  $1.10 \times$  to  $4.73 \times$  speedups with 1% to 2% accuracy degradation. Syno also accelerates GPT-2 training by  $1.1 \times$  and improves the language perplexity metric from 111 to 99. We also investigate the discovered operators and find novel and efficient semantics with interesting neural algorithm insights.

## 2 Background and Related Work

In this section, we briefly introduce the three most related concepts: neural architecture search, tensor compilers, and program synthesis, all of which can be used to better design and implement neural network operators.

### 2.1 Neural Architecture Search

As neural networks (NNs) are being applied to more and more domains, the needs of designing specific NN models are becoming increasingly prevalent. *Neural architecture search* (NAS) has emerged consequently to automatically design new model structures [8, 20, 42, 43], and indeed, many of the recently proposed models that showed state-of-the-art accuracy levels were discovered by NAS rather than manually crafted [28–30, 37]. NAS typically defines a highly modular search space by dividing the backbone model topology into basic units (called *cells*) of various sizes. It then proceeds to explore how to construct each cell by composing from several types of basic layers (a.k.a., *operators*) like convolutions, matrix multiplications (matmuls), and pooling. Throughout the search, the accuracy levels of the candidate cell structures are continuously evaluated. With such an automated flow, NAS is able to efficiently explore a much larger design space, and hence discover NN architectures with higher accuracy than manually designed models.

Besides solely focusing on accuracy, *performance-aware* NAS methods aim to strike a better balance between prediction accuracy and execution speed [2, 3, 29, 37]. Specifically, they inherit the design space from traditional NAS while integrating hardware efficiency metrics. By considering factors such as latency alongside accuracy, the search process could yield model architectures that are not only high-quality but also high-performance<sup>1</sup> on particular hardware.

We emphasize that both traditional and performance-aware NAS methods only *compose existing operators*, such as convolutions and matmuls, in a coarse-grained black-box way. Thus they are limited by these computationally expensive operators. The lack of flexibility to *invent novel operators* leaves ample opportunities for further optimizations, as we will demonstrate in this work.

### 2.2 Tensor Compilers

At the system level, an NN model is typically represented as a *tensor program*, in which the input/output and intermediate data are all cast as tensors, and a set of operators are applied to the tensor data to derive the final outcome. As a result, *tensor compilers* have recently gained great attention to accelerate NN execution, by applying general and specialized compile-time optimizations to compile the operator into high-performance *kernels*<sup>2</sup> [5, 24, 36, 39, 40].

Typically, kernels are written as loop nests, and each tensor compiler has its intermediate representation (IR) for describing and optimizing kernels. We here take Halide [24] as an example. Many tensor compilers use similar IR designs [5, 15, 32, 39]. Halide provides the separation of algorithm and schedule, where the algorithm is purely functional,

<sup>1</sup>Throughout this paper, we use “quality” for model accuracy, and “performance” for execution speed.

<sup>2</sup>We use *kernel* to represent a concrete implementation of an *operator*.

and the schedule dictates the concrete loop nest implementation involving tiling, vectorization, reordering, etc. For example, Listing 1 shows how we define a convolution in Halide, which is just simplified loop nests operating on specific dimensions (i.e., *coordinates*) of the tensors. With this IR, we can flexibly express different tensor computations.

```
auto [r_Ci, r_K_H, r_K_W] = RDom(0, C_in, 0, K, 0, K);
out(i_N, i_Co, i_H, i_W) +=
  input(i_N, r_Ci, i_H + r_K_H - K / 2, i_W + r_K_W - K / 2)
  * weight(i_Co, r_Ci, r_K_H, r_K_W);
```

**Listing 1.** The conv2d operator represented in Halide.

The separation of algorithm and schedule enables tensor compilers to explore the optimization space that is *semantically equivalent* to the original program, i.e. the purely functional computation description as in Listing 1. This is in contrast to NAS-like approaches that find *semantically inequivalent* programs with better functionalities, so the two approaches are *orthogonal*. Turner et al. [35] extended tensor compilers, relaxing the equivalence constraint to apply *inequivalent* transformations on loop nests in tensor programs to realize NAS. However, their approach pre-defined only a few simple inequivalent transformations, such as grouping and bottlenecking the range of a loop, thus only exploring a limited search space still in the scope of traditional operators.

### 2.3 Program Synthesis

Program synthesis is an approach that automatically generates a program that complies with several *specifications*, such as a set of input and output example pairs, or a set of assertions [11]. Theoretically speaking, the general concept of program synthesis can be applied to design new NN operators, but there exist several practical gaps. Traditional program synthesis only treated *correctness* as the target, such as TF-Coder [27] that synthesizes TensorFlow code to help programmers write correct code. But NN models, which are known to tolerate small errors, do not have a clear notion of correctness, while the goal is to improve inference accuracy. Also, existing program synthesis approaches can hardly scale, currently only limited to consider highly constrained program space. The complexity of loop nests in typical NN operators is well beyond their capabilities. We discuss these challenges in more detail in Section 3.

$\alpha$ NAS [17] relaxed the correctness objective to apply goal-directed program synthesis for NAS. They applied transformations to subgraphs in the model, which could generate new operators beyond traditional NAS. But they are still constrained by traditional operators like convolutions and matmuls, so the potential of intra-operator program synthesis remains unexploited. As a result, their speedups were light, as Section 9 will show. Ma et al. [21], on the other hand, pre-defined some fine-grained primitives common in traditional demosaicking pipelines to perform NAS, however they did not allow freely exploring new operators, either.

## 3 Motivation and Challenges

In this work, we aim to automatically and efficiently synthesize novel NN operators from very basic atoms in programming languages, with the hope of discovering new operators that have both high accuracy quality and high execution performance. Such automatic *neural operator synthesis* is highly profitable. State-of-the-art models today such as transformers and convolutional networks rely heavily on operators like attention and convolution that are constructed based on human insights. Automatic discovery of such operators can potentially create more promising model architectures.

**Comparison with existing paradigms.** Neural operator synthesis has a similar goal to performance-aware NAS, but aims to synthesize tensor programs at a much more fine-grained level rather than directly composing known operators like convolutions and matmuls. More specifically, operator synthesis involves writing various loop nests and the tensor expressions in the loop body. For example, for the convolution in Listing 1, the loops are implicitly defined by the iterators (*i\_Co*, *r\_Ci*, etc.), and the tensor expressions are realized with the *coordinate expressions*. Coordinate expressions are key to an operator because they specify how tensor elements are arranged and which are involved in the computation. Here, the simple addition of iterators (*i\_H + r\_K\_H*) implies convolution, and the repeated uses of the reduction iterator (*r\_Ci*) in two tensors imply contraction (a.k.a., tensor multiplication). The rich semantics of coordinate expressions can be exploited to synthesize novel operators. We note that such operator synthesis is impossible under existing NAS. Although it is always possible to lower existing operators to nested loops, it is *not* always possible to do the inverse. If a loop nest cannot be decomposed into several existing operators, it is likely we have discovered a novel operator.

On the other hand, operator synthesis is also significantly different from tensor compilers. Existing tensor compilers mostly preserve the semantic equivalence as discussed in Section 2.2. Thus they are unable to discover *new* operators. Actually, in operator synthesis, we deliberately avoid the exploration of semantically equivalent operators (see Section 6). If we synthesize equivalent operators, we would be very likely to redo those existing optimizations in tensor compilers. In this sense, *tensor compilers and operator synthesis are orthogonal*. We first synthesize novel operators, and then leverage tensor compilers to optimize its execution performance on the particular hardware.

We view neural operator synthesis as a specialized form of program synthesis in the NN domain. While traditional synthesis methods are limited to simple programs, we need to handle more complex operators with various nested loop structures and coordinate expressions. On one hand, the degree of freedom in directly writing loop nests and tensor expressions is huge, leading to an extremely large search space. On the other hand, as in performance-aware NAS, for

each candidate operator, we need to assess both its accuracy level and execution speed, both of which require substantial time. To measure the accuracy, we have to use real datasets to train the full NN model for several epochs at least. Several theoretical metrics are proposed to predict the accuracy potential with minimum training cost [1, 19, 34, 41], but we find them to perform poorly in reality, especially for irregular operators we aim to construct. To evaluate the speed, we need to generate an optimized implementation of the operator on real hardware. This could also cost significant time in state-of-the-art tensor compilers [5, 24, 40].

**Challenges.** We highlight three main challenges in neural operator synthesis that distinguish it from traditional program synthesis. First, with traditional program synthesis, the loop nest (e.g., Listing 1) can be enumerated with bottom-up search, building the coordinate expressions from the atoms such as iterators and constants [11]. The main issue of this generic approach is the difficulty of ensuring *high quality* for NN operators, due to the lack of high-level semantics. For example, if we fill the indices of input with all 0s, all other elements would be discarded, which is not at all reasonable. An NN operator is usually expected to satisfy certain properties, such as differentiability, full utilization of input data elements, etc., so that it can be trained in an NN model and achieve good accuracy. Encoding such constraints into inputs to an SMT solver may be possible, but would be too slow and expensive when searching over a huge number of operator candidates.

Second, a major issue of exploring the search space is *redundant operators*, which exhibit the same or *similar* semantics and show similar quality and performance. For example, in integer arithmetic, there is an identity  $B*i/(B*C)=B*(i/C)$ . Our synthesis needs to skip these equivalent coordinate expressions. Moreover, even inequivalent expressions can induce similar computation: consider iterators  $i, j$  with domains  $B, K$  where  $B > C \gg K$ , then  $(i+j)/C=i/C$  holds for almost every point. Traditionally, the redundancy can be handled with term rewrite systems [22] and equality saturation [33], but this slows down the search, and also cannot prune away inequivalent but similar expressions.

Third, conventional program synthesis has developed multiple approaches to guide the synthesis with user-provided specifications to eliminate illegal candidates [11]. With neural operators, the only correctness constraint is that the input and output tensor shapes must match with those specified by the model. However, under the aforementioned quality constraints, the domains of coordinate expressions cannot be freely altered to match the input and output shapes, making randomly sampled operators almost always illegal in terms of tensor shapes. Thus, we need a specially designed novel approach to *guide the synthesis process*.

In summary, to realize practical neural operator synthesis, we must design a framework with the properties below.

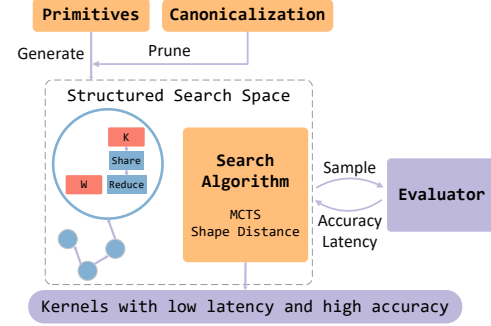


Figure 1. Overview architecture of Syno.

- **High quality.** Synthesized operators need to satisfy certain properties (e.g., differentiability, full data utilization), similar to existing NN operators.
- **No redundancy.** Repeated evaluation of operators with the same or similar semantics should be avoided. Particularly, we should not redo the optimizations in existing tensor compilers.
- **Guided search.** The synthesis process should be guided by the input and output tensor shapes to improve search efficiency.

## 4 Design Overview

We propose Syno, an end-to-end, automatic, and efficient framework for neural operator synthesis. Given a backbone NN model, Syno is able to synthesize novel linear operators with high quality (for accuracy) and high performance (for speed), which can be a drop-in replacement of the original operators (convolution, matmul, etc.) with the same input and output tensor shapes. The model topology and the non-linear activation layers are unaltered. Specifically, given the input and output tensor shapes, e.g.,  $[N, C_{in}, H, W]$  and  $[N, C_{out}, H, W]$  for convolution, or  $[M, K]$  and  $[M, N]$  for matmul, Syno discovers novel operators that satisfy the accuracy and performance requirements, e.g., best performance with less than 1% accuracy loss. Note that the tensor shapes are specified as symbolic variables to allow one operator to fulfill different tensor sizes. The framework also supports a rich set of user-defined budgets such as FLOPs, memory usage, and number of parameters.

We limit our search in Syno to linear operators. First, linear operators are usually the performance bottleneck in NNs, constituting most of the computations, so reducing their complexity can have great gains. Second, non-linear activation layers like ReLU provide the non-linearity needed in NNs, so we keep them unaltered in the backbone model. Their performance impact is negligible because they can be readily fused into the previous operators by tensor compilers.

---

**Algorithm 1** Workflow of Syno.

---

```

1: procedure SEARCH(model, dmax)
2:   kernels  $\leftarrow$  EXTRACTKERNELS(model)
3:   substs  $\leftarrow$  SYNTHESIZESUBSTITUTIONS(kernels, dmax)
4:   for all subst  $\in$  MCTS(substs) do
5:     model'  $\leftarrow$  REPLACE(model, kernels, subst)
6:     accuracy  $\leftarrow$  TRAINWITHPYTORCH(model')
7:     if IsWITHINACCURACYMARGIN(accuracy) then
8:       performance  $\leftarrow$  TUNEWITHTVM(model')
9:       output subst, accuracy, performance

10: function SYNTHESIZESUBSTITUTIONS(kernels, dmax)
11:   input, output  $\leftarrow$  SYMBOLICSHAPE(kernels)
12:   results  $\leftarrow$  {}
13:   procedure ENUMERATE(d, n)
14:     if HASMATCHINGSHAPE(n, input) then
15:       Add n to results if within budgets
16:     if d  $\geq$  dmax then return
17:     for all n'  $\in$  ENUMERATECHILDREN(n) do
18:       Backtrack with shape distance.
19:       if SHAPEDISTANCE(n', input)  $>$  dmax - d - 1 then
20:         continue
21:       ENUMERATE(d + 1, n')
22:     ENUMERATE(0, ROOTNODE(output))
23:   return results

25: function ENUMERATECHILDREN(n)
26:   children  $\leftarrow$  {}
27:   for all prim  $\in$  ENUMERATEPRIMITIVES(n) do
28:     if IsCANONICAL(n, prim) then Canonicalize.
29:       children  $\leftarrow$  children  $\cup$  {ADD(n, prim)}
30:   return children

```

---

Algorithm 1 outlines the overall workflow of Syno, which is also illustrated in Figure 1. Syno relies on a library of *fine-grained primitives* that operate on specific tensor *coordinates*, i.e., dimensions (Section 5). A new operator candidate is synthesized by iterative sampling and adding new primitives (Algorithm 1 Lines 27 to 29), until a maximum size (Line 17). Compared to directly composing arbitrary coordinate expressions, using these primitives ensures high quality with tensor semantics and enables efficient structured search, while not sacrificing expressiveness.

Since our primitives are defined on tensor coordinates, we can directly apply *expression simplification* and *canonicalization* techniques for coordinate expressions to quickly eliminate redundant candidates (Algorithm 1 Line 28), enabling efficient design exploration. Our canonicalization rules not only remove most equivalent operators during the search but can also prune those with similar semantics (Section 6).

To efficiently discover valid operators, we guide the synthesis flow using a novel metric of *shape distance*, which is the distance between the current partial operator and the boundary conditions, i.e., input/output tensor shapes to

match. We then leverage the intrinsic structure of the design space and formalize the search as a stochastic decision process to apply the Monte Carlo Tree Search algorithm (Section 7). The discovered operators are then fed to the two code generators targeting PyTorch and TVM [5], for accuracy and performance evaluations, respectively (Section 8).

Syno is implemented as a distributed infrastructure, which could leverage multiple GPUs across several server nodes to conduct searches, particularly accelerating model training. Syno has 19K lines of C++ code and 11.5K lines of Python.

## 5 Primitives

Syno adopts a novel approach to synthesize candidate operators from a set of fine-grained primitives, whose semantics are defined with *tensor coordinate expressions* in a bottom-up way, as shown in Table 1. Compared with directly enumerating arbitrary raw arithmetic expressions as abstract syntax trees (ASTs) of integer expressions, this allows us to perform synthesis and search with the primitives in a more structured manner to ensure high quality.

### 5.1 Structured ASTs

Synthesizing expressions in a bottom-up way, i.e., first specifying the innermost atoms and then composing them, is common in program synthesis [11]. This is also a natural choice for NN operators. As can be seen in Listing 1, the output tensor are indexed by the output iterators such as *i\_H*, and the coordinate expressions comprising the output iterators, e.g., *i\_H* + *r\_K\_H* - *K*/2, are used to index the input tensors. Thus a straightforward way is to use the output iterators as atom coordinate expressions and enumerate more complicated expressions as the indices of input tensors.

However, the operators synthesized in this way tend to have *low quality*. For example in Listing 1, if *i\_Co* were only used in an expression *i\_Co* / 2, then every two consecutive channels of *out* would have identical feature maps. This means tensor elements are replicated, and we perform redundant computations. To avoid this, we can require that *i\_Co* % 2 must also be present in the enumerated coordinate expressions. This example inspires us to design a *high-quality* primitive that transforms a coordinate expression [*i*] with domain [N] to two coordinate expressions [*i* / *B*, *i* % *B*] of domains [N / *B*, *B*] where *B* divides *N*. Formally we write: [*i*]: [N]  $\leftarrow$  [*i* / *B*, *i* % *B*]: [N / *B*, *B*].

Furthermore, this *bottom-up primitive* also has *top-down semantics*, namely to flatten a tensor of shape [N / *B*, *B*] into [N] by merging the two dimensions. We name it as MERGE, which is actually a common *tensor view operation*. A view is just another way of accessing a tensor, and we identify that various arithmetic operations (+, \*, /, etc.) on tensor coordinates actually correspond to views. For example, the addition of coordinate expressions is equivalent to extracting neighbor elements, which is UNFOLD. Similarly, adding a

**Table 1.** Syno primitives that transform coordinate expressions and their domains in a bottom-up way. For example, UNFOLD combines two coordinates with domains N and K, and obtains an expression of domain N (with out-of-bound elements clipped), while its top-down semantics are to extract sliding windows of size K from the coordinate of domain N.

Class	Primitive	Parameter	Bottom	Top	Top-Down Semantics
Views	SPLIT	-	$[i, j]: [G, B]$	$\leftarrow [B * i + j]: [G * B]$	Partition into blocks
	MERGE	B	$[i]: [N]$	$\leftarrow [i / B, i \% B]: [N / B, B]$	Flatten two dimensions
	SHIFT	-	$[i]: [N]$	$\leftarrow [(i + 1) \% N]: [N]$	Shift along a dimension
1-to-many	EXPAND	-	$[i]: [C]$	$\leftarrow []: []$	Repeat or up-sample
	UNFOLD	-	$[i, j]: [N, K]$	$\leftarrow [i + j - K/2]: [N]$	Extract sliding windows
many-to-1	STRIDE	S	$[i]: [K]$	$\leftarrow [S * i]: [S * K]$	Strided access
Contractions	REDUCE	N	$[]: []$	$\leftarrow \sum_i [i]: [N]$	Reduce a dimension
	SHARE	-	$[i]: [N]$	$\leftarrow ([i], [i]): ([N], [N])$	Element-wise product

constant is SHIFT, multiplication is SPLIT and STRIDE, and discarding an expression is EXPAND. We summarize them in the class of views in Table 1. All of them except EXPAND and STRIDE do not discard or replicate elements and thus have high quality. The two low-quality primitives could be useful for special cases such as up-sampling and dilated convolution. For semantic completeness, we keep them but limit their occurrences in each synthesized operator.

Aside from coordinate expressions that extract elements from tensors, we need primitives to actually perform the computation. For now, we only support linear operations in Syno, so elements from multiple tensors are multiplied and summed up. The reductions (RDom in Listing 1) can be abstracted to a primitive REDUCE, which adds a sum reduction loop. Meanwhile, a SHARE primitive indexes two tensors with the same coordinate expression, and performs multiplication between the two tensors. The top-down semantics of REDUCE and SHARE are mainly *tensor contraction operations*. A contraction involves combining two tensors along a certain dimension [10], e.g., the input channels of input and weight tensors are contracted in Listing 1.

With this approach, we propose a structured way of using the Syno primitives to build coordinate expression ASTs for neural operators. An operator composed in this way has a very similar structure to common ASTs, except that instead of trees, expressions are now determined by direct acyclic *primitive graphs* (pGraphs). Figure 2 shows how to compose a 2D convolution of Listing 1 using Syno primitives. The vertices are the primitives, while the edges are (possibly intermediate) coordinate expressions, and can be evaluated in the same way as we evaluate ASTs. We can implement many PyTorch operators such as nn.Conv2d, nn.Fold, nn.AvgPool2d, nn.PixelShuffle in Syno.

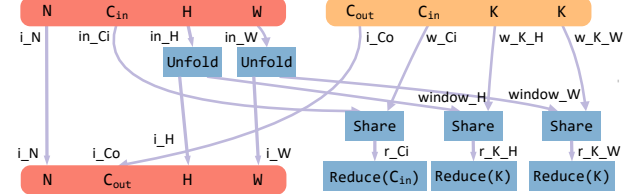


**Figure 2.** The pGraph of conv2d in Syno.

## 5.2 Advantages

The structured bottom-up primitives in Syno present several advantages. First, they ensure *high quality* of synthesized operators, in that they are differentiable [14] and do not discard input data or replicate data. The only relatively low-quality EXPAND and STRIDE are restrictively used and STRIDE is required to be paired with 1-to-many primitives to ensure the high-quality property. Second, they allow *structured search*. With the primitives, similar pGraphs are likely to share a subgraph, which makes the search space highly structural and enables the use of effective search algorithms (Section 7.2). Third, the primitives are *expressive*, as they are devised based on most basic arithmetic operations on coordinate expressions.

## 5.3 Design Details

To match an operator with different concrete input/output tensor shapes, and to support additional parameter variables in some primitives (e.g., MERGE needs a factor B), Syno uses *symbolic shapes* when synthesizing operators. We further split the symbols into two classes. *Primary variables* are for input/output dimensions, e.g.,  $C_{out}$ ,  $H$ . They are relatively large and thus are not allowed to appear in the denominator of a coordinate expression. *Coefficient variables* are only introduced by primitives, and are relatively small and allowed to appear in denominators. When enumerating the applicable primitives on a partial pGraph, the primitive parameters

are represented by monomials of primary variables and coefficient variables, with the degrees (i.e., powers) limited within a user-specified range. Syno replaces the variables with concrete sizes at code generation.

In the current prototype of Syno, we only consider operators that process a single input tensor (not including weights) and produce a single output tensor, and disallow multiple uses of the same (input or intermediate) tensors such as residual links [12]. This restriction seems strict, but in fact existing operator types like convolution, matmul, and pooling all satisfy it. We argue that the lost flexibility is usually more critical at the full model graph level rather than the operator level. Our operators can still be plugged into arbitrary model topologies including ResNet [12], where the residual links are realized outside the operator. We plan to extend Syno to support multiple input tensors in the future.

## 6 Canonicalization

The design space of synthesizing operators from our primitives is extremely large, with a lot of redundant operator constructs, especially those that can be readily discovered by tensor compilers. Take the partial pGraph [Figure 3\(a\)](#) as an example. In the left side, the topmost coordinate expressions are given by  $[i, j]$ :  $[A*B, C] \xleftarrow{\text{SPLIT}} [C*i+j]$ :  $[A*B*C]$ .  $\xleftarrow{\text{MERGE}(B*C)} [(C*i+j)/(B*C), (C*i+j)%(B*C)]$ :  $[A, B*C]$ . However, this simplifies to  $[i/B, C*(i\%B)+j]$ , corresponding to the right side  $[i, j]$ :  $[A*B, C] \xleftarrow{\text{MERGE}(B)} [i/B, i\%B, j]$ :  $[A, B, C] \xleftarrow{\text{SPLIT}} [i/B, C*(i\%B)+j]$ :  $[A, B*C]$ .

To improve search efficiency, Syno uses a set of *canonicalization rules* to filter out uncanonical redundant candidates on the fly when new primitives are added to partial pGraphs (IsCANONICAL in [Algorithm 1](#) Line 28). Syno does *not* aim to eliminate *all* redundancies, which is highly challenging, if not impossible, considering the rich primitive semantics. Also, comprehensive canonicalization checks are extremely expensive and sometimes undecidable [22]. On the other hand, Syno supports canonicalization rules to skip operators with *similar computation results*. We also note that the canonicalization rules in Syno are easily *extensible*. Developers can define new rules and plug them into the framework.

**Contractions.** Since weight tensors can be arbitrarily reshaped offline, there is no need to apply views to weights. Thus weight coordinates are directly used in SHARES for contractions. Moreover, since SHARE is symmetric, we always put weight coordinates as the right-hand-side inputs of SHARES.

**Between views and contractions.** We enforce a canonical order between views and contractions. The 1-to-1 views do not involve actual computations so they can be freely swapped with contractions. We thus *push down* all 1-to-1 views after contractions, as in [Figure 3\(b\)](#).

For the others, we apply rules to avoid doing futile work. For example, we disallow combining EXPAND and REDUCE because this only changes a multiplier of the result; UNFOLD allows at most one output coordinate to be REDUCED.

**Between two views.** Most redundancies exist between views because of the many primitive types. The key to their canonicalization is *to apply expression simplification techniques*. In many tensor compilers such as Halide [24] and TVM [5], expressions are simplified before analysis and lowering. In Syno, as our primitive definitions are based on coordinate expressions, we can similarly simplify the coordinate expressions corresponding to the (sub)pGraph consisting of view primitives, and the fully simplified expression gives the canonical form. For example, the aforementioned [Figure 3\(a\)](#) is one such example, where the right side is simplified and thus canonical, corresponding to the rule that a MERGE cannot be above a SPLIT.

We design expression simplification in Syno by referring to Halide’s term rewrite system (TRS) [22]. TRS sequentially substitutes the terms in an AST from bottom to top with pattern matching in expressions, in order to obtain the simplified form [22]. In our pGraph, each coordinate (edge) is like an AST node. We treat the bottom outputs of a subgraph as wildcards and match the top input expressions against the patterns. Again look at [Figure 3\(a\)](#). The bottom outputs are marked as  $[\#0, \#1]$ . Then the substitution can be formulated as  $[(C*\#0+\#1)/(B*C), (C*\#0+\#1)%(B*C)] \rightarrow [\#0/B, C*(\#0\%B)+\#1]$ , which is a pattern-matching-based rewrite rule. To choose the canonical (i.e., “simplest”) form among equivalent expressions, we empirically define simplicity as removing parentheses as much as possible by applying distribution laws of multiplication, division, and modulo. We can see [Figure 3\(a\)](#) removes one level of parentheses. Following this approach, we derive a series of rewriting rules involving multiple primitives.

In addition, it is better to not just canonicalize semantically equivalent subgraphs, but also eliminate candidates with only slightly different semantics, so that a wider range of semantics can be explored with fewer samples. In [Figure 3\(c\)](#), on the left side, with  $[i, j]$ :  $[A*B, K]$  as the output coordinates, the inputs are  $[(i+j-K/2)/B, (i+j-K/2)\%B]$ :  $[A, B]$ . If B is much larger than K as in most convolutions, then  $j-K/2$  is much less than B. So we can simplify the expressions to  $[i/B+j-K/2, i\%B+j-K/2]$  as the right side, which is equal to the left-hand side at almost every point. These approximately equivalent rules can also be implemented with TRS-based rules as above. They effectively enable us to only synthesize operators that are significantly distinct.

## 7 Guided Search

We next describe the overall synthesis and search process in Syno. [Section 7.1](#) discusses the bottom-up synthesis approach. A critical challenge is how to ensure the exact match

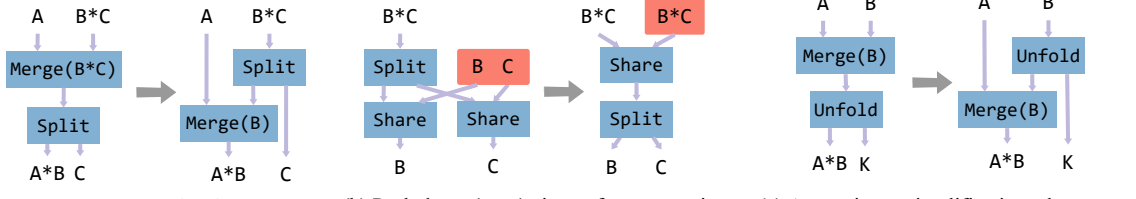


**Figure 3.** Examples of some canonicalization rules used in Syno.

of input/output tensor dimensions with the given specification. We propose a novel concept of shape distance to guide the search process. Section 7.2 explains our specific search algorithm based on Monte Carlo Tree Search (MCTS) [6, 9, 13].

### 7.1 Bottom-Up Synthesis with Shape Distance

As mentioned in Section 5, Syno performs bottom-up synthesis, starting from the output coordinates and iteratively applying sampled primitives for a limited number of steps. For example, as a subgraph of Figure 2, from output  $[i\_H]$ :  $[H]$ , we can get  $[i\_H]$ :  $[H] \xleftarrow{\text{REDUCE}(K)} [i\_H, r\_K\_H]: [H, K] \xleftarrow{\text{SHARE}} ([i\_H, r\_K\_H], [r\_K\_H]): ([H, K], [K]) \xleftarrow{\text{UNFOLD}} ([i\_H + r\_K\_H - K / 2], [r\_K\_H]): ([H], [K])$ . The weight ( $[K]$  here) does not need to be transformed further (Section 6), so we use the term *shape* to refer to the shape of the first tensor (data input), which is  $[H]$  in this case.

The data tensor shape of a complete pGraph should match exactly with the specified input shape (*input* in Algorithm 1 Line 12). While synthesizing with primitives ensures high quality, it also becomes hard to control the shape of the coordinates after applying primitives on a partial pGraph. Ideally, after flexibly exploring various primitives, when the partial pGraph gets close to its maximum size limit, the last few primitives need to move towards exactly matching with the input dimensions. For example, if the shape of the current partial pGraph is  $[C_{in}, s^{-1}*H, s*W, k]$ , we can apply  $[C_{in}, s^{-1}*H, s*W, k] \xleftarrow{\text{MERGE}} [C_{in}, s^{-1}*H, s, W, k] \xleftarrow{\text{UNFOLD}} [C_{in}, H, W, k] \xleftarrow{\text{MERGE}} [C_{in}, H, W]$ .

We propose a novel metric named *shape distance* as the minimum number of required primitives added onto the current pGraph to reach the input. In the above example, the shape distance of  $[C_{in}, s^{-1}*H, s*W, k]$  is 3. If the remaining allowed number of primitives is less than the shape distance, we can immediately terminate the current pGraph and backtrack (Algorithm 1 Line 20). This avoids deviating too far from the input coordinates.

We design a systematic method in Syno to compute the shape distance between the current shape and the desired input. We first divide the coordinates in the two shapes into *reshape groups*, where future primitives are only applied to the coordinates within each group to match them, but not across groups. In the above example, we can have three

reshape groups, as  $\{C_{in}\} \leftarrow \{C_{in}\}$ ,  $\{s^{-1}*H, s*W\} \leftarrow \{H, W\}$ ,  $\{k\} \leftarrow \{\}$ . Reshape groups can be decided by comparing the primary variables in the coordinate expressions. When there exist multiple possible grouping schemes (but usually only a few), we enumerate all and find the least distance.

We then compute the distance within each reshape group. We identify the *helpful primitives* that will help in shape matching: reshape primitives (i.e., MERGE, SPLIT) which regroup dimensions, and 1-to-many primitives (i.e. UNFOLD, EXPAND) which eliminate dimensions. If the left-hand side and the right-hand side of the reshape group have the same size of domains, e.g.,  $\{s^{-1}*H, s*W\}$  and  $\{H, W\}$  have domains of  $H*W$ , then we only need to regroup dimensions, using SPLIT and MERGE. In this case we only need 2 steps:  $[s^{-1}*H, s*W] \xleftarrow{\text{MERGE}} [s^{-1}*H, s, W] \xleftarrow{\text{SPLIT}(s)} [H, W]$ . We can prove a generalized conclusion of  $\#lhs + \#rhs - 2$  steps, where  $\#lhs$  and  $\#rhs$  are the numbers of dimensions in the left-hand and right-hand sides of the reshapes (both are 2 in this example). On the other hand, if the two sides have different sizes of domains, then at least one 1-to-many primitives is required, in which case totally  $\#lhs + \#rhs - 1$  steps are needed. Summing the steps required in all reshape groups yields an upper bound for shape distance. Then, all grouping schemes are enumerated, and backtracking is used to find the minimum of the upper bounds, which yields the final shape distance. The detailed algorithm and proof are provided in the appendix.

When the input involves repeated coordinates, e.g.,  $[C_{in}, H, H]$  for square images, we enumerate all possible permutations, allowing tensor transpose during final matching.

### 7.2 MCTS-Based Search

Our search algorithm is based on MCTS. We formulate our search problem as a Markov decision process, where we transit from one partial pGraph to another in the search space, with the action space being the primitives. The final states are complete pGraphs. The optimization goal is operators with both high accuracy and high inference speed. Given that operators with high accuracy are much less than those with high speed, we set a hard upper limit for FLOPs and use accuracy as the reward for MCTS to guide it to learn how to find expressive operators within a given FLOPs budget. We

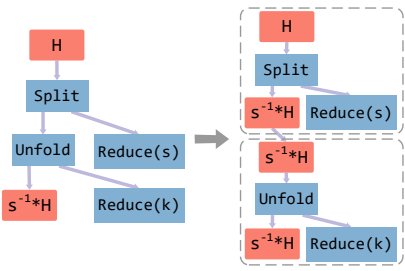


Figure 4. An example of rfactor optimization.

record all MCTS samples and filter out operators with bad accuracy to obtain the final result.

## 8 Code Generation

We implement two code generators for accuracy and speed evaluations, respectively. First, a *PyTorch code generator* is built to make use of the already highly-tuned operator libraries for training. Using the top-down semantics, each view primitive is lowered to its counterpart in PyTorch, and each contraction primitive is lowered to an einsum [25] expression, which is a general method for performing tensor contractions. The primitives are lowered in the topological order to ensure that dependencies are satisfied.

Although the PyTorch approach is fast in compilation, it lacks compile-time optimizations such as operator fusion and other tiling schemes. We further build a *TVM code generator*, following the bottom-up semantics, to evaluate all coordinate expressions according to the kernel graph, and leverage TVM [5] for extensive compiler optimizations on specific hardware, e.g., our mobile CPUs and GPUs in Section 9.

Some optimization passes unique to Syno are designed. An important one aims to automatically insert intermediate stages to eliminate redundant computation. Consider the example in Figure 4. A trivial code generator creates a loop nest of  $(H/s)*k*s$  iterations computing  $Y[i] = \sum_{i_k} \sum_{i_s} X[i + i_k - k/2 + s*i_s]$  as in the left side, but this is mathematically equivalent to  $Z[i'] = \sum_{i_s} X[i' + s*i_s]$ ,  $Y[i] = \sum_{i_k} Z[i + i_k - k/2]$ , which corresponds to the partitioned subgraphs on the right. By doing so we reduce the FLOPs from  $k*H$  to  $(1+k/s)*H$ .

Generally speaking, FLOPs depend only on the output dimensions and the REDUCES, which are the spatial loops and reduction loops in the loop nest. The number of iterations is their product. In the case of 1-to-many primitives like UNFOLD, the output dimensions are increased, so if we perform any REDUCE after this, FLOPs are unnecessarily increased because we are evaluating  $k$  copies for each element.

This issue is unique to the Syno IR. We propose an optimization called *rfactor*, i.e., factorization of reduction domain, to deal with it. We enumerate the order of performing reductions, i.e., the order of lowering each REDUCE. If a REDUCE

is lowered, only the primitives that can reach that REDUCE are required to be lowered. In the example, the SPLIT and the UNFOLD can both reach the bottom REDUCE, but only the 1-to-many UNFOLD cannot reach the upper REDUCE. So the upper REDUCE is prioritized to form a subgraph.

## 9 Evaluation

### 9.1 Experimental Setups

**Hardware configurations.** Our operator search and accuracy validation are done on a cluster with NVIDIA A100 GPUs. For performance in edge-device inference scenarios, we test the end-to-end latency on NVIDIA Jetson Orin Nano 8 GB, which features a 6-core Arm Cortex-A78AE mobile CPU and a 1024-core NVIDIA Ampere GPU with 32 tensor cores. This device is well-suited for model inference at the edge.

**Workloads.** We mainly focus on vision tasks with five popular vision NNs: ResNet-18 [12], ResNet-34 [12], DenseNet-121 [16], ResNeXt-29-2x64D [38], and EfficientNet-V2-S [31]. We aim to substitute all standard convolutions in them. To prove the wide adaptability of Syno, we also test GPT-2 [23] (117M parameters with 12 layers, 12 heads, and 768 embedding dimensions) by substituting its QKV projections.

**Baselines.** We use three baselines for the comparison of vision tasks. TVM MetaSchedule [26] is a state-of-the-art tensor compiler that performs automatic tuning. Comparing to it is fair since Syno also uses a TVM code generator. Turner et al. [35] (labeled as NAS-PTE) is the first to introduce loop-level transformations into NAS, and  $\alpha$ NAS [17] is the first to apply program synthesis for NAS albeit at a coarse granularity. Because the search and tuning methods of NAS-PTE are not open-sourced, we compare with their operators on individual layers instead of full models.  $\alpha$ NAS neither open-source their search results nor provide inference performance, so we only compare with their FLOPs and training speedups reported in the original paper. For GPT-2, we evaluate the training speed relative to the original model.

**Datasets and training configurations.** ImageNet [7] is unsuitable for directly searching because of its large size, so we use the smaller yet still challenging CIFAR-100 [18] as the proxy dataset. Specifically, during the search Syno trains the NN model using each candidate operator for 100 epochs on CIFAR-100. The selected best operators are then fully trained on ImageNet for 90 epochs for accuracy and performance evaluation. We scale the CIFAR-100 images to the same size as ImageNet to ensure the same inference performance. For GPT-2, we employ the language perplexity (PPL) metric on the LM1B Benchmark [4]. The data type for both training and inference is FP32. The training hyperparameters for the optimizer and learning rate scheduler are dataset-dependent to ensure reasonable accuracy, but they are not heavily tuned.

**Computation cost.** Training a model on CIFAR-100 for 100 epochs takes two to three hours. In our experiments, we

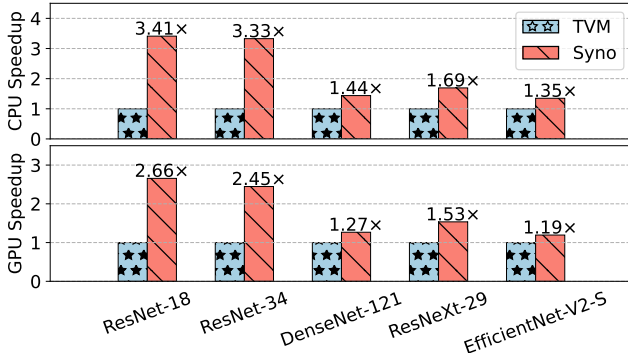


**Figure 5.** End-to-end performance comparison between Syno and the TVM baseline on CIFAR-100.

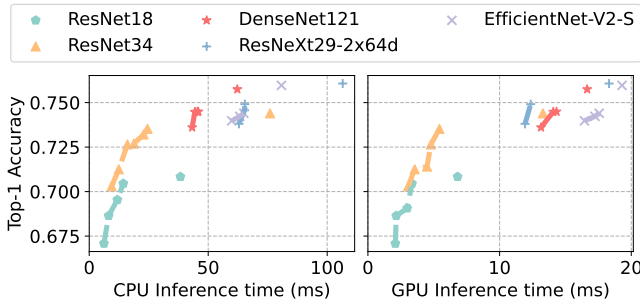


**Figure 6.** Pareto optimal curves of accuracy vs. inference time between Syno and the TVM baseline on ImageNet. For each model, the standalone point is the baseline, and the connected points are discovered by Syno.

terminate early when the accuracy is not as high as expected, thereby reducing the average evaluation computation cost to 0.1 GPU hours per sample. We spend roughly 300 GPU hours per model.

## 9.2 Results on Vision Tasks

For vision tasks, we search for the fastest operators in each model with less than 1% accuracy loss, a commonly used threshold. We separately target both CPUs and GPUs.

**CIFAR-100 results.** Figure 5 shows the best operators we find in terms of inference latency. On the CPU (GPU) of our edge device, Syno achieves 2.06 $\times$  (1.72 $\times$ ) speedup on average (geomean), and up to 3.41 $\times$  (2.66 $\times$ ) across all workloads, compared to TVM-compiled baselines. Syno performs better on traditional NNs like ResNet-18 due to the discovered novel operators. Even for NAS-optimized models such as EfficientNet-V2, Syno can still achieve a performance gain of 1.35 $\times$  (1.19 $\times$ ). We analyze the benefits of our novel discovered operators in detail below.

**ImageNet results.** For every model, we select some discovered operators that have comparable accuracy with the baseline and re-evaluate them on ImageNet. We plot the

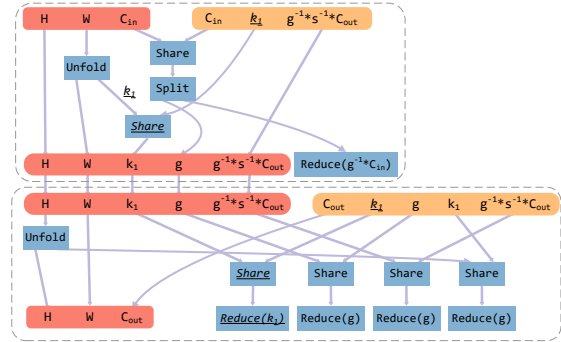


**Figure 7.** OPERATOR 1 discovered by Syno.

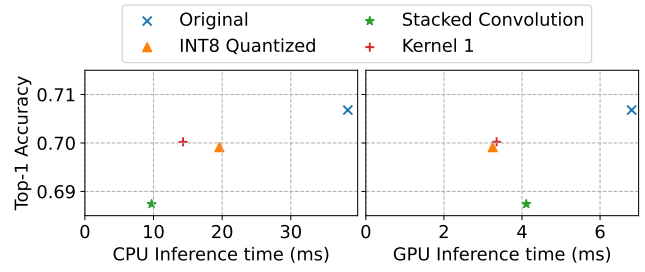


**Figure 8.** Comparison between OPERATOR 1 and other optimizations. Accuracy evaluated on ImageNet.

Pareto optimal curves of accuracy vs. inference time in Figure 6. Most of our operators exhibit a minor 1% to 2% accuracy loss while enabling 1.10 $\times$  to 4.73 $\times$  speedups. If more accuracy loss is acceptable, then going along the Pareto curves further boosts performance.

We highlight a comparison between our optimized ResNet-34 and the baseline ResNet-18. Replacing the standard convolutions with our operators in ResNet-34 results in a model with *both* higher accuracy and better inference time than the ResNet-18 baseline. This observation implies a potentially promising direction to extend Syno to accuracy-preserving NN optimization: users can stack more layers and then compress the model with Syno, which might result in better accuracy and lower latency at the same time.

**Case studies.** Among all the operators discovered, we find two convolution-like operators with outstanding accuracy, inference performance, and superior expressiveness.

OPERATOR 1 shown in Figure 7 achieves 2 $\times$  speedup with less than 1% ImageNet accuracy degradation. After the rfactor optimization during code generation (Section 8), it becomes a stack of two stages *similar to* 1D and 2D grouped convolutions, but is *not* expressible in NAS. NAS can only sample traditional (grouped) convolutions, which always perform contraction between unfolded windows of spatial dimensions and weights (the standard  $\sum_j X[i + j - K / 2] * W[j]$  pattern). However, in OPERATOR 1, the first stage

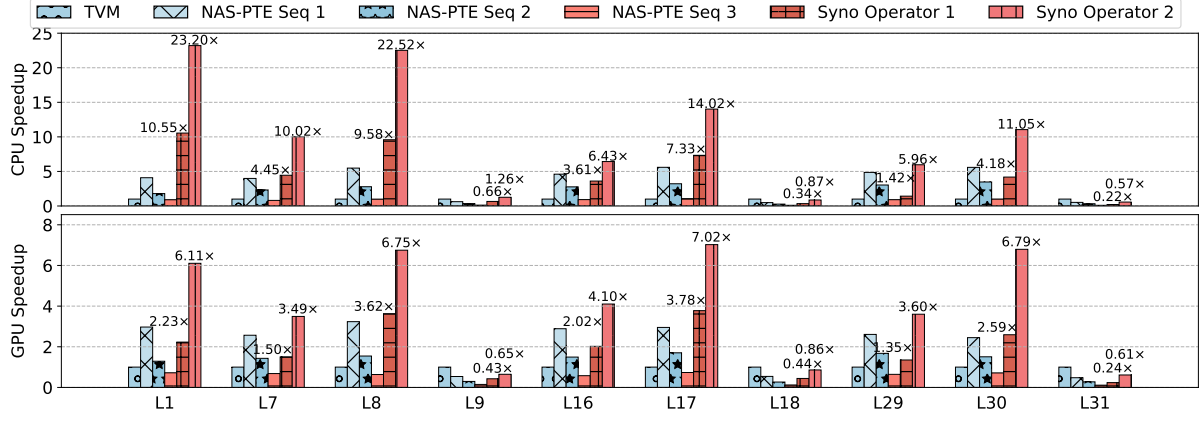


**Figure 9.** Layer-wise performance comparison between Syno and NAS-PTE on ResNet-34.

breaks this limitation. See the pattern underscored and italicized in Figure 7, which comprises 2 SHARES, 1 REDUCE, and 3 coordinates with domain  $k_1$ . The SHARE in the first stage would have been REDUCED, had it been a traditional convolution. But the UNFOLDED window remains and is passed to the second stage to be contracted with the weight.

To see why such a pattern is effective, we stack two grouped convolutions into an operator, which is just OPERATOR 1 with the SHARED  $k_1$  in stage 1 REDUCED and  $W$  in stage 2 UNFOLDED again (hence may be discoverable under traditional NAS schemes). As in Figure 8, although having the same FLOPs and similar latency, stacked convolution has doubled the accuracy degradation, which we attribute to the difference in the receptive field in OPERATOR 1 ( $3 \times 3$  vs.  $3 \times 5$ ) that eases training of the model. This may provide insights for the machine learning community.

To further compare with other optimization techniques that trade accuracy for performance, we choose INT8 quantization. As in Figure 8, OPERATOR 1 has slightly better accuracy than INT8 quantization, as well as lower latency on the CPU. Note that Syno-synthesized operators can also be quantized, so the two techniques can be applied jointly to further enhance performance.

OPERATOR 2 is a variant of OPERATOR 1, and resembles two 1D convolutions with weights connected using SHARE in a similar manner. Benefiting from the weight SHARE-ing, OPERATOR 2 yields  $3.41 \times$  ( $2.66 \times$ ) speedup with a reasonable accuracy decrease (within 1% on CIFAR-100). We attribute the substantial performance speedup to its fewer parameters (less than 1/4 of standard 2D convolution) that can fit in the limited caches on edge devices.

**Comparison with NAS-PTE.** Figure 9 shows the layer-wise performance of OPERATOR 1 and OPERATOR 2 compared to TVM and all the three operators proposed by NAS-PTE, when used in ResNet-34. On the CPU (GPU), the two novel operators outperform the traditional convolution by  $2.25 \times$  ( $1.30 \times$ ) and  $5.35 \times$  ( $2.84 \times$ ) on average, and up to  $23.20 \times$  ( $7.02 \times$ ). Compared to NAS-PTE, the speedup of our best

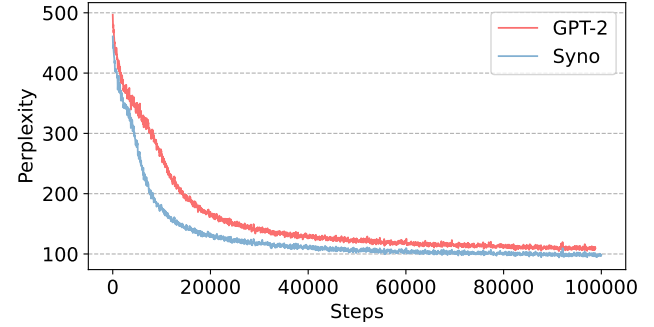


**Figure 10.** Comparison of language perplexity vs. training steps between Syno and the original GPT-2.

operators over their best ones is  $2.13 \times$  ( $1.68 \times$ ) on average. our best operators reduce FLOPs by  $1.76 \times$  to  $4.32 \times$ , and reduce the number of parameters by  $1.80 \times$  to  $9.50 \times$ . These improvements are achieved without any layer-wise tuning like NAS-PTE but by a fully automated workflow in Syno.

**Comparison with  $\alpha$ NAS.**  $\alpha$ NAS reported FLOPs reduction ratios and training speedups for some variants of ResNet and EfficientNet. Within 2% ImageNet accuracy drop,  $\alpha$ NAS achieves 25% fewer FLOPs and about 12% training speedup on both ResNet-50 and EfficientNet-B0, while Syno achieves 63% and 37% fewer FLOPs and 178% and 17% GPU inference speedup on ResNet-34 and EfficientNet-V2-S, respectively. This qualitatively shows Syno’s advantages over  $\alpha$ NAS.

### 9.3 Results on GPT-2

We follow Primer [28] to allocate a 30-minute training period on GPT-2 for each searched operator and compare their final language perplexity results. We then extend the training for the best-performing operator and the original model to reach 100,000 steps as shown in Figure 10. When searching for substitutions for the QKV projection, our best operator achieves a  $1.1 \times$  training speedup and reduces the perplexity to 99, outperforming the original model’s perplexity of 111. More specifically, our operator constructs the original

**Table 2.** Canonical rates of different sampled pGraph sizes.

2	3	4	5	6	7	$\geq 8$
1.0000	0.1818	0.1397	0.0440	0.0122	0.0008	0.0000

projections by groups, which allows the QKV matrices used in the attention modules to learn from different features of input tokens, thereby improving the training efficiency.

#### 9.4 Ablation Studies

**Canonicalization.** To show the effectiveness of Syno canonicalization rules, we draw 6452 samples without canonicalization, among which only 86 are canonical. This implies that canonicalization cuts more than  $70\times$  redundancy. Table 2 shows the canonical rates for different pGraph sizes.

**Shape distance.** To check the effectiveness of the shape distance metric, we evaluate the successful rate of random sample trials with or without shape distance. On a server machine with 192 virtual cores, 253 distinct operators are found after 5 million trials in 68.33 seconds, with shape distance enabled. However, without the shape distance, 500 million trials in 180.51 seconds yield no valid operators. Thus, shape distance is vital for avoiding useless synthesis.

## 10 Conclusions

This paper advocates the paradigm of neural operator synthesis, which automatically discovers novel NN operators with good accuracy and performance. A practical framework named Syno has also been implemented, using a rich set of fine-grained primitives to construct operators, applying canonicalization to eliminate redundancy, guided by a distance metric to improve synthesis efficiency. Syno is able to discover better NN operators than existing ones on various models, with higher performance and minor accuracy loss.

## References

- [1] Mohamed S Abdelfattah, Abhinav Mehrotra, Łukasz Dudziak, and Nicholas D Lane. Zero-cost proxies for lightweight nas. *arXiv preprint arXiv:2101.08134*, 2021.
- [2] Hadjer Benmeziane, Kaoutar El Maghraoui, Hamza Ouarnoughi, Smail Niar, Martin Wistuba, and Naigang Wang. A comprehensive survey on hardware-aware neural architecture search. *arXiv preprint arXiv:2101.09336*, 2021.
- [3] Han Cai, Ligeng Zhu, and Song Han. Proxylessnas: Direct neural architecture search on target task and hardware. *arXiv preprint arXiv:1812.00332*, 2018.
- [4] Ciprian Chelba, Tomas Mikolov, Mike Schuster, Qi Ge, Thorsten Brants, and Philipp Koehn. One billion word benchmark for measuring progress in statistical language modeling. *Proceedings of the Annual Conference of the International Speech Communication Association, INTERSPEECH*, 12 2013.
- [5] Tianqi Chen, Thierry Moreau, Ziheng Jiang, Lianmin Zheng, Eddie Yan, Haichen Shen, Meghan Cowan, Leyuan Wang, Yuwei Hu, Luis Ceze, et al. {TVM}: An automated {End-to-End} optimizing compiler for deep learning. In *13th USENIX Symposium on Operating Systems Design and Implementation (OSDI 18)*, pages 578–594, 2018.
- [6] Rémi Coulom. Efficient selectivity and backup operators in monte-carlo tree search. In H. Jaap van den Herik, Paolo Ciancarini, and H. H. L. M. (Jeroen) Donkers, editors, *Computers and Games*, pages 72–83, Berlin, Heidelberg, 2007. Springer Berlin Heidelberg.
- [7] Jia Deng, Wei Dong, Richard Socher, Li-Jia Li, Kai Li, and Li Fei-Fei. Imagenet: A large-scale hierarchical image database. In *2009 IEEE conference on computer vision and pattern recognition*, pages 248–255. Ieee, 2009.
- [8] Thomas Elsken, Jan Hendrik Metzen, and Frank Hutter. Neural architecture search: A survey. *The Journal of Machine Learning Research*, 20(1):1997–2017, 2019.
- [9] Romaric Gaudel and Michele Sebag. Feature selection as a one-player game. In *Proceedings of the 27th International Conference on International Conference on Machine Learning, ICML’10*, page 359–366, Madison, WI, USA, 2010. Omnipress.
- [10] Werner Greub. *Multilinear Algebra*. Springer, Berlin, 1978.
- [11] Sumit Gulwani, Oleksandr Polozov, Rishabh Singh, et al. Program synthesis. *Foundations and Trends® in Programming Languages*, 4(1-2):1–119, 2017.
- [12] Kaiming He, Xiangyu Zhang, Shaoqing Ren, and Jian Sun. Deep residual learning for image recognition. In *Proceedings of the IEEE conference on computer vision and pattern recognition*, pages 770–778, 2016.
- [13] Yu-Jhen Hsu and Diego Perez Liebana. MCTS Pruning in Turn-Based Strategy Games. In *AIIDE-20 Workshop on Artificial Intelligence for Strategy Games*, 2020.
- [14] Shi-Min Hu, Dun Liang, Guo-Ye Yang, Guo-Wei Yang, and Wen-Yang Zhou. Jittor: a novel deep learning framework with meta-operators and unified graph execution. *Science China Information Sciences*, 63:1–21, 2020.
- [15] Yuanming Hu, Tzu-Mao Li, Luke Anderson, Jonathan Ragan-Kelley, and Frédéric Durand. Taichi: a language for high-performance computation on spatially sparse data structures. *ACM Transactions on Graphics (TOG)*, 38(6):1–16, 2019.
- [16] Gao Huang, Zhuang Liu, Laurens Van Der Maaten, and Kilian Q Weinberger. Densely connected convolutional networks. In *Proceedings of the IEEE conference on computer vision and pattern recognition*, pages 4700–4708, 2017.
- [17] Charles Jin, Phitchaya Mangpo Phothilimthana, and Sudip Roy. Neural architecture search using property guided synthesis. *Proceedings of the ACM on Programming Languages*, 6(OOPSLA2):1150–1179, 2022.
- [18] Alex Krizhevsky, Geoffrey Hinton, et al. Learning multiple layers of features from tiny images. 2009.
- [19] Namhoon Lee, Thalaiyasingam Ajanthan, and Philip HS Torr. Snip: Single-shot network pruning based on connection sensitivity. *arXiv preprint arXiv:1810.02340*, 2018.
- [20] Chenxi Liu, Barret Zoph, Maxim Neumann, Jonathon Shlens, Wei Hua, Li-Jia Li, Li Fei-Fei, Alan Yuille, Jonathan Huang, and Kevin Murphy. Progressive neural architecture search. In *Proceedings of the European conference on computer vision (ECCV)*, pages 19–34, 2018.
- [21] Karima Ma, Michael Gharbi, Andrew Adams, Shoaib Kamil, Tzu-Mao Li, Connelly Barnes, and Jonathan Ragan-Kelley. Searching for fast demosaicking algorithms. *ACM Transactions on Graphics (TOG)*, 41(5):1–18, 2022.
- [22] Julie L Newcomb, Andrew Adams, Steven Johnson, Rastislav Bodik, and Shoaib Kamil. Verifying and improving halide’s term rewriting system with program synthesis. *Proceedings of the ACM on Programming Languages*, 4(OOPSLA):1–28, 2020.
- [23] Alec Radford, Jeff Wu, Rewon Child, David Luan, Dario Amodei, and Ilya Sutskever. Language models are unsupervised multitask learners. 2019.
- [24] Jonathan Ragan-Kelley, Connelly Barnes, Andrew Adams, Sylvain Paris, Frédéric Durand, and Saman Amarasinghe. Halide: a language and compiler for optimizing parallelism, locality, and recomputation

in image processing pipelines. *ACM SIGPLAN Notices*, 48(6):519–530, 2013.

[25] Alex Rogozhnikov. Einops: Clear and reliable tensor manipulations with einstein-like notation. In *International Conference on Learning Representations*, 2021.

[26] Junru Shao, Xiyou Zhou, Siyuan Feng, Bohan Hou, Ruihang Lai, Hongyi Jin, Wuwei Lin, Masahiro Masuda, Cody Hao Yu, and Tianqi Chen. Tensor program optimization with probabilistic programs. *Advances in Neural Information Processing Systems*, 35:35783–35796, 2022.

[27] Kensen Shi, David Bieber, and Rishabh Singh. Tf-coder: Program synthesis for tensor manipulations. *ACM Transactions on Programming Languages and Systems (TOPLAS)*, 44(2):1–36, 2022.

[28] David R So, Wojciech Marnik, Hanxiao Liu, Zihang Dai, Noam Shazeer, and Quoc V Le. Primer: Searching for efficient transformers for language modeling. *arXiv preprint arXiv:2109.08668*, 2021.

[29] Mingxing Tan, Bo Chen, Ruoming Pang, Vijay Vasudevan, Mark Sandler, Andrew Howard, and Quoc V Le. Mnasnet: Platform-aware neural architecture search for mobile. In *Proceedings of the IEEE/CVF Conference on Computer Vision and Pattern Recognition*, pages 2820–2828, 2019.

[30] Mingxing Tan and Quoc Le. Efficientnet: Rethinking model scaling for convolutional neural networks. In *International conference on machine learning*, pages 6105–6114. PMLR, 2019.

[31] Mingxing Tan and Quoc Le. Efficientnetv2: Smaller models and faster training. In *International conference on machine learning*, pages 10096–10106. PMLR, 2021.

[32] Shizhi Tang, Jidong Zhai, Haojie Wang, Lin Jiang, Liyan Zheng, Zhen-hao Yuan, and Chen Zhang. Freetensor: a free-form dsl with holistic optimizations for irregular tensor programs. In *Proceedings of the 43rd ACM SIGPLAN International Conference on Programming Language Design and Implementation*, pages 872–887, 2022.

[33] Ross Tate, Michael Stepp, Zachary Tatlock, and Sorin Lerner. Equality saturation: a new approach to optimization. In *POPL ’09: Proceedings of the 36th annual ACM SIGPLAN-SIGACT symposium on Principles of Programming Languages*, pages 264–276, New York, NY, USA, 2009. ACM.

[34] Jack Turner, Elliot J Crowley, Michael O’Boyle, Amos Storkey, and Gavin Gray. Blockswap: Fisher-guided block substitution for network compression on a budget. *arXiv preprint arXiv:1906.04113*, 2019.

[35] Jack Turner, Elliot J Crowley, and Michael FP O’Boyle. Neural architecture search as program transformation exploration. In *Proceedings of the 26th ACM International Conference on Architectural Support for Programming Languages and Operating Systems*, pages 915–927, 2021.

[36] Haoji Wang, Jidong Zhai, Mingyu Gao, Zixuan Ma, Shizhi Tang, Liyan Zheng, Yuanzhi Li, Kaiyuan Rong, Yuanyong Chen, and Zhihao Jia. {PET}: Optimizing tensor programs with partially equivalent transformations and automated corrections. In *15th USENIX Symposium on Operating Systems Design and Implementation (OSDI 21)*, pages 37–54, 2021.

[37] Bichen Wu, Xiaoliang Dai, Peizhao Zhang, Yanghan Wang, Fei Sun, Yiming Wu, Yuandong Tian, Peter Vajda, Yangqing Jia, and Kurt Keutzer. Fbnet: Hardware-aware efficient convnet design via differentiable neural architecture search. In *Proceedings of the IEEE/CVF conference on computer vision and pattern recognition*, pages 10734–10742, 2019.

[38] Saining Xie, Ross Girshick, Piotr Dollár, Zhuowen Tu, and Kaiming He. Aggregated residual transformations for deep neural networks. In *Proceedings of the IEEE conference on computer vision and pattern recognition*, pages 1492–1500, 2017.

[39] Jie Zhao, Bojie Li, Wang Nie, Zhen Geng, Renwei Zhang, Xiong Gao, Bin Cheng, Chen Wu, Yun Cheng, Zheng Li, et al. Akg: automatic kernel generation for neural processing units using polyhedral transformations. In *Proceedings of the 42nd ACM SIGPLAN International Conference on Programming Language Design and Implementation*, pages 1233–1248, 2021.

[40] Lianmin Zheng, Chengfan Jia, Minmin Sun, Zhao Wu, Cody Hao Yu, Ameer Haj-Ali, Yida Wang, Jun Yang, Danyang Zhuo, Koushik Sen, et al. Ansor: Generating {High-Performance} tensor programs for deep learning. In *14th USENIX Symposium on Operating Systems Design and Implementation (OSDI 20)*, pages 863–879, 2020.

[41] Dongzhan Zhou, Xinchu Zhou, Wenwei Zhang, Chen Change Loy, Shuai Yi, Xuesen Zhang, and Wanli Ouyang. Econas: Finding proxies for economical neural architecture search. In *Proceedings of the IEEE/CVF Conference on computer vision and pattern recognition*, pages 11396–11404, 2020.

[42] Barret Zoph and Quoc V Le. Neural architecture search with reinforcement learning. *arXiv preprint arXiv:1611.01578*, 2016.

[43] Barret Zoph, Vijay Vasudevan, Jonathon Shlens, and Quoc V Le. Learning transferable architectures for scalable image recognition. In *Proceedings of the IEEE conference on computer vision and pattern recognition*, pages 8697–8710, 2018.

## A Shape Distance

Here we provide a formal proof for the shape distance formulation.

First, we provide some technical details. The process of matching the dimensions in a partial pGraph to the input tensor is called *finalization*. The dimensions in a partial pGraph that belong to the data tensor are called *finalizable dimensions*, meaning that they may be used to finalize. For example, in the conv2d pGraph, if we just ignore the batch size N, then right before finalization, the topmost dimensions in the partial pGraph is  $([C_{in}, H, W], [C_{out}, C_{in}, K, K])$ , and the finalizable dimensions are just  $[C_{in}, H, W]$ .

The construction of a pGraph is separated into several stages, where each stage only samples specific kinds of primitives. Basically, there are *Reduction Stage*, *Normal Stage*, and *Contraction Stage*. In the Reduction Stage, only REDUCES are generated. In the Contraction Stage, only SHARE can be generated, and we define a helper primitive CONTRACTION to generate all needed SHARES for a contraction with a weight tensor, and assign all the needed dimensions to the weight tensor. We here note that CONTRACTION is a 1-to-many primitive, in that it may assign some dimensions to the weight tensor, reducing the number of elements in the finalizable dimensions. Normal Stage generates all the other primitives. To construct a pGraph, there is only 1 Reduction Stage which generates all the required REDUCES, and then the Normal Stage and Contraction Stage are performed alternately. The conv2d pGraph can be constructed in 3 stages, namely:

$$\begin{aligned}
 & \text{Reduction Stage } [C_{out}, H, W] \xleftarrow{\text{REDUCE}(C_{in}), \text{REDUCE}(K), \text{REDUCE}(K)} \\
 & [C_{out}, H, W, C_{in}, K, K], \text{Contraction Stage } [C_{out}, C_{in}, \\
 & H, W, K, K] \xleftarrow{\text{CONTRACTION}} ([C_{in}, H, W, K, K], [C_{out}, C_{in}, \\
 & K, K]), \text{ and Normal Stage } ([C_{in}, H, W, K, K], [C_{out}, \\
 & C_{in}, K, K]) \xleftarrow{\text{UNFOLD}, \text{UNFOLD}} ([C_{in}, H, W], [C_{out}, C_{in}, K, \\
 & K]). \text{ The finalizable dimensions change from } [C_{out}, H, W] \\
 & \text{to } [C_{out}, H, W, C_{in}, K, K] \text{ to } [C_{in}, H, W, K, K] \text{ to } [C_{in}, H, W].
 \end{aligned}$$

The greatest rationale for the separation of stages is that the number of elements in the shape of the partial pGraph (recall that we only consider the finalizable dimensions, ignoring the weights), or *numel*, defined as the product of all the finalizable dimensions, *decreases monotonically* in all the stages except the initial Reduction Stage. First consider contractions. A dimension transformed by a CONTRACTION either goes to both the data tensor and the weight tensor, so *numel* is constant, or goes to the weight tensor, so *numel* is reduced. In the previous example,  $[C_{in}, K, K]$  go to both the data tensor and the weight tensor, and  $[C_{out}]$  goes to the weight tensor. Then the views. The only many-to-1 primitives are REDUCE and STRIDE. After the Reduction Stage, there is no REDUCE, and since we do not allow discarding data, STRIDED dimensions are not finalizable, and must be transformed as an UNFOLD RHS. For other 1-to-1 views and 1-to-many views, clearly *numel* decreases or remains constant after each application.

Now we introduce *helpful primitives* based on the monotonicity of *numel*. Since we want to compute *the minimum required steps for finalization*, any primitive that does not help reduce the required steps can be ignored. Clearly SHIFT can be ignored because it does not change the shape. STRIDE does not help either, because it requires an UNFOLD to be applied later, which can be applied without the STRIDE. So the helpful primitives are: reshapes (SPLIT, MERGE), and 1-to-many primitives (EXPAND, UNFOLD, CONTRACTION). The reshapes fuse or factor finalizable dimensions, and 1-to-many primitives eliminate 1 or more finalizable dimensions.

**Definition A.1.** *Extended finalization.* For a specific set of finalizable dimensions, a subgraph in a (not yet determined) pGraph is called an extended finalization if it only includes helpful primitives, and takes the input shape as input, and the specified finalizable dimensions as output.

An extended finalization is a speculated set of primitives from the current finalizable dimensions to the desired input shape. The lower bound of all speculations is clearly the result.

**Definition A.2.** *The shape distance of a specific set of finalizable dimensions is the minimum of the number of primitives of all possible extended finalizations.*

Clearly we cannot simply enumerate all extended finalizations, which is equivalent to exhaustively expanding the search space. So, with these facts, we further define the notion of *reshape groups*. We can actually simplify helpful primitives. All we need to know about helpful 1-to-many primitives is that, they eliminate 1 or more finalizable dimensions, and actually we only need these semantics, as we are only concerned with shapes. So we remove UNFOLDS, connecting the input and output LHS, adding an EXPAND to output RHS; remove CONTRACTIONS, connecting the input LHS and output of SHARES, ignoring the weights (dimensions that only

go to weights now instead are connected to EXPANDS). Then we obtain an extended finalization with only reshapes and EXPAND. We name this *simplified extended finalization*.

**Definition A.3.** *Reshape groups.* The reshape groups of an extended finalization are the connected components of its corresponding simplified extended finalization.

An intuitive explanation for this is the dimensions in a reshape group are fused and later factored, so as to match the corresponding desired input dimensions. In the previous example, the output/input pairs of the reshape groups are  $\{C_{in}\} \leftarrow \{C_{in}\}$ ,  $\{s^{-1} * H, s * W\} \leftarrow \{H, W\}$ ,  $\{K\} \leftarrow \{K\}$ .

**Theorem A.1.** *In a reshape group with input/output pair  $I, O$ , and let the dimensions eliminated by 1-to-many primitives be  $E$ . Then the number of SPLITS #SPLIT is at least  $|O| - 1$ , and the number of MERGES #MERGE is at least  $|I| + |E| - 1$ . Moreover,  $\#SPLIT - |O| = \#MERGE - |I| - |E|$ .*

*Proof.* Since the eliminated dimension has no input, they resemble input dimensions a lot. So let  $I, E \leftarrow I \cup E, \emptyset$ , and we only need to prove for the case where there is no EXPAND. There are only MERGES and SPLITs, and the application of each MERGE increases finalizable dimensions by 1, and each SPLIT decreases it by 1.

We start from the current finalizable dimensions  $O$  and go step by step. At first there are  $O$  connected components (because there are only the output dimensions). Each MERGE does not affect the connected components because it just adds to a component. Each SPLIT either acts on a connected component, or combines 2 connected components into a single one. So the number of connected components in the last is at least  $|O| - \#SPLIT$ . By definition, a reshape group is connected, so  $|O| - \#SPLIT \leq 1$  and we get  $\#SPLIT \geq |O| - 1$ . The proof for the inequality for #MERGE is similar. And we only need to track the number of finalizable dimensions to get the “moreover” part.  $\square$

The input and output pairs of reshape groups are independent of the detailed extended finalization, and only dependent on the current finalizable dimensions and the desired dimensions.

**Theorem A.2.** *Let the input, eliminated and output dimensions of the reshape groups of an extended finalization be  $\{(I_i, E_i, O_i)\}_i$ . Then the shape distance is at least  $\sum_i (|I_i| + |O_i| - 2)$  if all  $E_i$ s are empty, and 1 more if any  $E_i$  is not empty.*

*Proof.* By theorem A.1, there are at least  $\sum_i (|I_i| + |O_i| - 2)$  reshape primitives. If there are any dimensions to be eliminated, a CONTRACTION may be enough.  $\square$

Now we only need to enumerate the reshape groups. The enumeration is not arbitrary, because the *numel* in the input dimensions is less than or equal to that in the output dimensions. We first enumerate the primary variables (N, C, H, W) and then perform appropriate backtracking. The implemented shape distance algorithm is very efficient.